VALIDATION PROCESS OF THE ICC DIGITAL CAMERA

R. Alamús, W. Kornus, V. Palà, F. Pérez, R. Arbiol, R. Bonet, J. Costa, J. Hernández,
J. Marimon, M.A. Ortiz, E. Palma, M. Pla, S. Racero, J. Talaya

Institut Cartogràfic de Catalunya, Parc de Montjuïc, 08038 Barcelona, Spain – ralamus@icc.es

ABSTRACT:

In 2004 the Institut Cartogràfic de Catalunya (ICC) decided to enter the world of aerial digital cameras with the aim to set up a totally digital workflow without loss of image quality.

Once the Digital Mapping Camera (DMC) of ZEISS / INTERGRAPH (Z/I) company was selected and delivered to the ICC a camera acceptance phase was carried out. The major goal of the acceptance phase was to check the performance of the DMC and to test the image quality (both geometric and radiometric) in comparison to an analog photogrammetric camera. Several projects have been flown in a dual camera configuration (analog and digital) in December 2004. The comparisons include urban flights with a GSD (Ground Sampling distance) of 8 cm (Amposta block), a block with a GSD of 50 cm (Caro block) and some images over two resolution targets with GSDs of 8 cm and 16 cm.

The Amposta block consisted in 5 parallel strips and 2 transversal strips taken from 800 m flight altitude. This block was already flown and aerotriangulated by the ICC in 2000 at a photo scale 1:5000 using an RC30 and B/W film so an urban map was available. GPS/INS data were used as aerial control in the block aerotriangulation. For different comparison purposes the block was aerotriangulated manually and also automatically.

The Caro block consisted in a 2 parallel strip project over a half plain and half mountainous area. It forms part of a larger block flown with a RC30 camera in summer 2004. Its main feature is that terrain height differences of up to 1000 m occur in one single image. The block images were taken with some clouds above the airplane. Digital images were compared to analog images taken simultaneously in December 2004 and to analog images taken in summer 2004 in good illumination conditions. From the DMC images an automatic DEM (Digital Elevation Model) was generated and compared to a reference DTM.

The resolution of the images was judged by means of two Siemens Star patterns having a size of 5x10m and 10x10m with a different number of sectors and which were imaged in different focal plane positions. Thus a possible loss of resolution near the edges of the image could be evaluated.

The paper analyses and discusses the DMC camera performance in terms of image resolution and accuracy of automatically derived DEMs. Finally conclusions are drawn from that investigation.

1. INTRODUCTION

In 2004 the Institut Cartogràfic de Catalunya (ICC) decided to go for a totally digital mapping workflow. Once the selection phase for a digital camera finished, a Digital Mapping Camera (DMC) of ZEISS / INTERGRAPH (Z/I) was delivered to the ICC. After that, ICC got the need to validate whether the DMC fulfils the ICC requirements for a camera for mapping proposes.

In this paper, test flights designed for camera validation are described and the DMC camera performance at different stages of the mapping workflow is analyzed and discussed including the comparison with corresponding results derived from analog cameras.

2. VALIDATION FIELD DESCRIPTION

2.1 Airborne equipment layout

The test areas have been flown with a dual camera configuration. The ICC Cessna Caravan airplane was carrying the ICC DMC camera (number 14 of the DMC series) and a RC30 with a 153 mm focal length. The IMU of an Applanix POS DG system was installed inside the DMC.

2.2 Amposta Block

The Amposta block consisted in 139 images which are distributed in 5 parallel strips and 2 transversal strips taken from 800 m flight altitude above ground, which means an 8 cm GSD. The block contains 7 full ground control points, 6 check points and 139 GPS/INS aerial control points.

2.3 Caro Block

The Caro block is a 2 parallel strip project (originally 3, but only 2 of them have been aerotriangulated). It was flown at 50 cm GSD over a terrain, which is half plain and half mountainous. The main feature of this block is that there is a large difference in height, which can reach 1000 m in one single DMC image. It forms part of a larger block flown with a film RC30 camera in summer 2004 at photo scale 1:30000.

The block was aerotriangulated with manual point identification. The DMC images were tied to the larger block flown and already aerotriangulated with the RC30. GPS/INS data were used as aerial control for DMC images in the Bundle Block Adjustment.

2.4 Resolution test

In order to evaluate the performance in terms of resolution several DMC images were taken over resolution targets. These targets are a 36-sector Siemens Star printed on a 10x10 m^2 canvas and a portion of an 11-sector Siemens Star printed on a 5x10 m^2 canvas.

Several images were taken over the targets at different positions of the focal plane and at heights of 800 and 1600 meters. Those images were taken with the digital and the analog cameras at the same time.

3. ANALYSIS OF RESULTS

In this section the performance of the DMC camera in different stages of mapping production workflow (aerotriangulation, DTM/DSM extraction and stereoplotting) as well as resolution are analysed using the data sets described above. All these subjects are compared against analog image data sets and derived products.

The analog images simultaneously taken in December 2004 in a dual camera configuration have only been used in resolution tests. Due the bad illumination conditions in that time of the year the quality of the analog images resulted poor, or at least poorer than usual. Therefore the analysis on aerotriangulation, DSM and stereoplotting was done with analog images taken in summer 2000 (Amposta) and summer 2004 (Caro) under good illuminating conditions.

3.1 Aerotriangulation

On the Amposta block it has been performed manual and automatic aerotriangulations, which are compared to the manual aerotriangulation carried out in 2000.

In the DMC block 2757 photogrammetric observations were measured corresponding to 431 tie points, 7 full ground control points and 6 check control points. 139 full GPS/IMU aerial control points have been used in the block adjustment. No self-calibration parameters have been used. The photogrammetric model used in the adjustment is described in (Baron et al., 2003).

Using Match-AT of the Inpho company 17068 photogrammetric observations of 3068 tie points were obtained from the same control and check points configuration. All 3D data are referred to projective UTM coordinates. Since Match-AT is exclusively working with Cartesian coordinates, the bundle block adjustments was carried out – like in all the other cases of that study - with the in house ACX-GeoTex software (Colomina et al., 1992) and Match-AT was used for the automatic production of photogrammetric observations only.

The analog block consists of 69 images distributed in 5 parallel strips and 2 transversal strips (as the DMC block above) with 1188 photogrammetric observations of 217 tie points, 8 full control points and 1 check point. 69 GPS aerial control points, one set of linear drift per strip and one set of self-calibration parameters have been used in the block adjustment.

The first topic to analyse is the point measurement accuracy applying semi-manual point identification in analog and DMC images as well as digital image matching in the DMC images. Table 1 shows that the pointing accuracy is improved by a factor of 1.3 comparing the manual point identification of DMC and analog images and even by a factor of 3 comparing digital image matching in DMC images to manual point identification in analog images.

	Analog 2000		DMC manual		DMC MatchAT	
	μm	pix.	μm	pix.	μm	pix.
x	4.83	0.32	2.85	0.24	1.23	0.10
y	4.27	0.29	2.35	0.20	1.12	0.09

Table 1. Photogrammetric residuals in μm and pixel considering the following three cases: Manual point identification in analog images flown in 2000 and scanned at 15 μm pixel size, manual point identification in DMC images and digital image matching (Match-AT) in DMC images

The second topic is the 3D point accuracy. Table 2 shows point accuracy at the 6 check points in the manual aerotriangulation. No significant differences were registered in the aerotriangulation with the automatically produced tie points. Notice that the image coordinates of check and control points always were measured manually. Unfortunately, the check points were not observed in the analog block in 2000 and therefore a comparison of the results is not possible for this set of data. Anyway, this topic is also analysed in the section 3.3 about stereoplotting accuracy with the DMC camera.

	Mean	R.M.S.	σ
X	-0.051 m	0.060 m	0.036 m
Y	0.008 m	0.018 m	0.018 m
H	-0.021 m	0.045 m	0.044 m

Table 2. Residuals at the 6 check points

Notice that these results are coherent with the predicted accuracies (1σ) of an aerotriangulation with DMC images, described in (Dörstel, 2003), which is 5 μm times the image scale in planimetry and 0.05 ‰ of the flying altitude in height. For the Amposta block this corresponds to 3 cm in planimetry and 4 cm in height.

Table 3 shows the internal point accuracy of the DMC block of Amposta. Notice that the values for the manually measured points match the expected accuracies referenced above. The automatically produced tie points are more accurate according to the higher image matching accuracy (see table 1).

	σ DMC manual	σ DMC Match-AT
# points	431	17068
X	0.03 m	0.01 m
Y	0.03 m	0.01 m
H	0.05 m	0.03 m

Table 3. Mean of the standard deviations over all tie points in the adjustment. On the left for the manual measured and on the right for the automatically produced tie points

After the application of the supplied image correction tools to remove geometric and radiometric distortions during the generation of the virtual image (Zeitler, 2002; Dörstel and Jacobsen, 2003), it was expected that the resulting digital images were free of geometric distortion. Nevertheless, a set of self-calibration parameters has been included in the adjustment of the automatic aerotriangulation of the Amposta block as it is suggested in (Dörstel, 2003). Figure 1 shows the effect of the estimated parameters. First of all notice that the used set of 12 Ebner self-calibration parameters (Ebner, 1976) are not appropriate since they do not take into account the 4-camera head-geometry of the DMC camera. Although 10 of the 12 parameters are estimated significantly (up to 35 times larger

than their standard deviation), they do neither improve the statistics of photogrammetric residuals nor other values in a significant manner, but they prove a systematic behavior of the photogrammetric residuals. Current investigation does not explain the cause of the error. It could be a miscalibration of the camera, a peculiarity of the block under study or a systematic tilt of the camera, which should introduce a different photo scale across-track in the image. Anyway, this effect will be investigated in further flights.
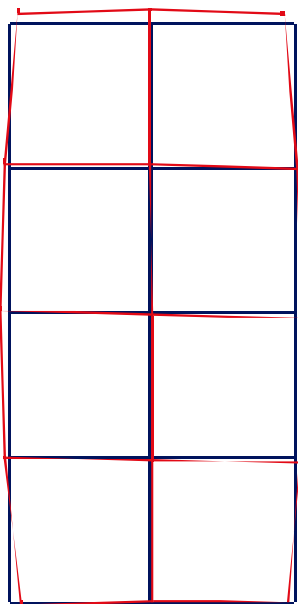

Figure 1. Effect of adjusted self-calibration parameters (in red) scaled by a factor of 1000

3.2 Automatic DSM

In order to assess the quality of automatic DSM generation a series of DSMs were produced both from the DMC images and from an overlapping subset of RC30 images of the Caro block described in section 2.3. Figure 2 shows the East-West orientation of the RC30 models, indicated in red, and the North-South orientation of the DMC models, indicated in blue color. The shaded relief representation of the corresponding DEM illustrates the separation between models lying in flat or mountainous terrain.
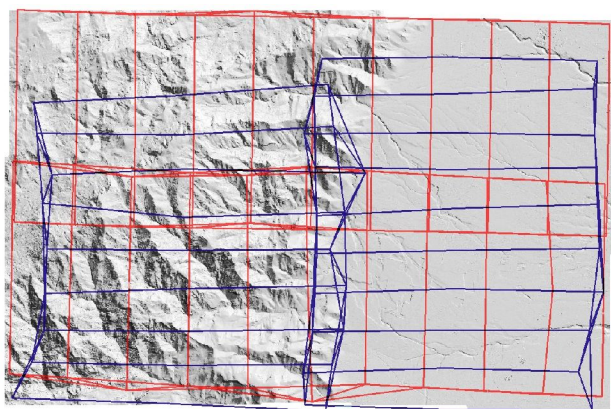

Figure 2: Location of the DMC models (blue) and of the RC30 models (red)

Altogether 70 models were calculated both from 80% and from 60% overlapping image pairs using the software package ISAE of the Z/I company (Krzystek, 1991). Since the DSM

generation accuracy decreases at the edges of the models the computation was restricted to an area, which is more or less included by the von Gruber positions of the respective image pair. The models were classified in 8 different categories (see table 4).

Camera	Overlap	Mountainous area	Flat area
DMC	60 %	7	8
	80 %	8	9
RC30	60 %	10	7
	80 %	11	9

Table 4: Number of calculated models in 8 categories

For each model a regular grid with 7.5 m spacing was produced. The grid point heights later were compared to the heights of an independent reference DTM with 1.1 m accuracy (1σ). Only 'good' grid points have been evaluated, i.e. points, marked by the ISAE software to be produced with low accuracy (< internally calculated threshold) or with low redundancy (<4) were excluded from the analysis.

The statistical results of the height comparison are listed in table 5. It must be stated, that this is a presentation of very first results and the actual test setup still contains important deficiencies. For instance, height differences between the surface model and the terrain model reflecting the heights of vegetation or buildings have not been filtered out. The accuracy of the reference DTM is of the same level as the investigated data and not of superior quality, as it should be. Therefore the results are just suitable to observe global tendencies and will not allow drawing final conclusions.

Camera	Overlap	b/h	Mountainous area			Flat area		
			mean	rms	σ	mean	rms	σ
DMC	60 %	0.31	1.6	3.8	3.4	1.3	1.9	1.2
	80 %	0.15	1.7	3.8	3.3	0.9	1.5	1.3
RC30	60 %	0.58	0.5	3.7	3.6	0.1	0.8	0.8
	80 %	0.29	0.9	4.3	4.2	0.3	1.0	0.9

Table 5: Statistics of height differences [m] between automatically derived DSM grid points and the reference DTM

It is well known, that the point height accuracy is directly related to the base to height (b/h) ratio and also to the point measurement accuracy. Although a smaller b/h ratio geometrically results in lower height accuracy, the smaller difference in the viewing angles on the other hand improves the point matching accuracy and also reduces the probability of occlusions in mountainous areas. Due to the smaller DMC image format in flight direction the b/h ratio just reaches approximately 50% of the b/h of a conventional frame camera like the RC30. According to the manufacturer of the DMC this accuracy loss is compensated by the higher quality of the digital DMC image and consequently by the higher point measurement accuracy (Dörstel, 2003). We could confirm this fact in a series of automatic aerotriangulation runs (Match-AT), which resulted in a σ_0 of approximately 0.1 pixel compared to approximately 0.3 pixel usually obtained with scanned conventional images.

Looking at the results in table 5 we observe a vertical shift between the DMC and the RC30 point heights of approximately 1 m. Since the effect of vegetation is not reduced, the reason

could be, that the DMC and RC30 images were taken in different seasons of the year. Generally the DMC point heights are determined with a slightly better accuracy in the mountainous area and worse accuracy in the flat area. It is curious, that the influence of the b/h ratio is not that visible.

	Theoretical values		Empirical results			
			Mountainous area		Flat area	
	DMC 60%	DMC 80%	DMC 60%	DMC 80%	DMC 60%	DMC 80%
RC30 60%	1.9	3.8	0.9	0.9	1.5	1.6
RC30 80%	0.9	1.9	0.8	0.8	1.3	1.4

Table 6: Relations between theoretical and empirical standard deviations for DMC and RC30 at 60% and 80% overlap

The columns 2 and 3 of table 6 show the relations of the theoretic height accuracies between DMC and RC30 as a function of their different b/h ratios assuming equal point measurement accuracy. In this sense the accuracies obtained with DMC images at 60% overlap are more or less comparable to RC30 images at 80% overlap (factor 0.9). If they are compared to RC30 at 60% the smaller b/h ratio of the DMC provokes 1.9 times less accurate point heights. The empirical results on the right side of table 6 reflect this situation only to some extent in the flat area. In the mountainous area the influence of the b/h ratio seems not to be reflected at all. This means that either the accuracy loss due to a smaller base length is compensated by a higher matching accuracy as mentioned above and/or the effect of vegetation and occlusions in the results and also the lack of a reference with superior accuracy is that important, that the geometric influence on the height accuracies does not become that visible. In a next step we will use a highly accurate laser scanner DSM as reference in order to reduce the effect of vegetation and buildings. So we will be able to draw more detailed conclusions from that analysis.

3.3 Stereoplotting

In this part of the analysis we have focused our efforts in the assessment of the accuracy in stereoplotting using DMC images.
Further work should investigate whether the capability of object detection increases with the DMC in comparison to analog cameras.

Firstly it is analyzed the accuracy of the system using ground control points, which were surveyed using GPS. Those ground points are stereoplotted using the digital camera images and analog camera images. In both cases the stereoscopic models were composed by images with 60% overlap. It must be noticed that we are comparing performance of digital camera with a b/h ratio of 0.3 against the analog camera with b/h ratio of 0.6. This analysis is carried out in the Amposta and Caro blocks, which have very different GSD: 0.08 m and 0.5 m respectively.

Tables 7 and 8 show the results of measuring 11 points in the Amposta block, and Tables 9 and 10 show the results of measuring 21 points in the Caro block.

# Points 11	X	Y	H
Mean	-0.05 m	0.03 m	-0.06 m
RMS	0.11 m	0.05 m	0.10 m

Table 7: Comparison between field data and stereoplotted data using digital camera images in the Amposta block

# Points 11	X	Y	H
Mean	-0.04 m	0.03 m	-0.04 m
RMS	0.10 m	0.10 m	0.07 m

Table 8: Comparison between field data and stereoplotted data using analog camera images in the Amposta block

# Points 21	X	Y	H
Mean	-0.06 m	-0.24 m	0.08 m
RMS	0.30 m	0.39 m	0.37 m

Table 9: Comparison between field data and stereoplotted data using digital camera images in the Caro block

# Points 21	X	Y	H
Mean	0.08 m	0.03 m	0.04 m
RMS	0.38 m	0.34 m	0.39 m

Table 10: Comparison between field data and stereoplotted data using analog camera images in the Caro block

Results, as have been seen in the DSM generation, show that smaller b/h ratio of the DMC camera is compensated, probably, due to the higher accuracy of the point measurement, reaching comparable accuracies in all components and the two different image scale data sets.

Secondly, a test was conducted to analyze in more detail the accuracy in height. Some points were collected in the common area of adjacent stereoscopic models close to the von Gruber points. Those points are stereoplotted in both adjacent models: along-track inside the same strip (table 11) and across-track between models in parallel strips (table 12).

	RMS RC30	RMS DMC
Adjacent models Amposta (53 points)	0.07 m	0.07 m
Adjacent models Caro (26 points)	0.30 m	0.30 m

Table 11: Comparison between adjacent models

	RMS RC30	RMS DMC
Adjacent strips Amposta (10 points)	0.08 m	0.10 m
Adjacent strips Caro (11 points)	0.30 m	0.65 m

Table 12: Comparison between adjacent strips

Table 11 shows that height determination is coherent along-track in both cases analog and digital. Nevertheless, table 12 comes up with degradation on the coherence in height determination across-track. These results show that in both blocks the accuracy in height has decreased in the case of the digital camera. Notice that the larger slope, in the transition from plain to mountainous terrain, is on the overlapping area between the DMC camera strips of the Caro block (see figure 2). Also, those overlapping areas are different in the analog models than in the digital as can be seen in figure 2. In future tests it must be checked whether this effect depends on the terrain features or, on contrary, is inherent to the DMC. In the latter case the self-calibration parameters that are shown in figure 1 can also be responsible of part of the error.

3.4 Image resolution

An automatic procedure has been set up at the ICC to measure the image resolution through the inspection of the 36-sector Siemens Star. The algorithm automatically detects the edges present in the image and adjusts a 3-D sigmoid that produces a resolution measure. Unfortunately, the size of the target (about 5 image pixels per sector) turned out to be insufficient for the

automatic procedure to run adequately. Instead, the same procedure has been applied in manual mode on the 11-sector target (figure 3). Five black and white different images from each camera have been used in the test. Further work has to compare resolution of DMC RGB images against film RGB ones.
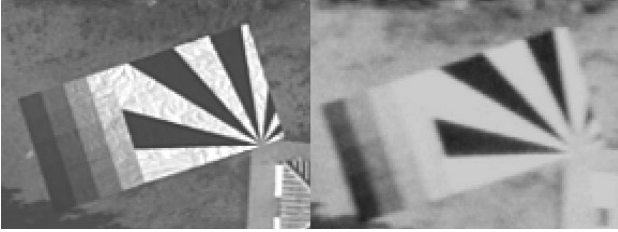

Figure 3. Digital (left) and analog (right) images of the 11-sector resolution target

First step is defining, on the images, the polygons that will be used to measure the edge. They must contain a good part of flat "white" and "black" areas so that the asymptotic branches of the sigmoid are well defined (see figure 4). This requirement prevents the use of the smaller sectors in our test.
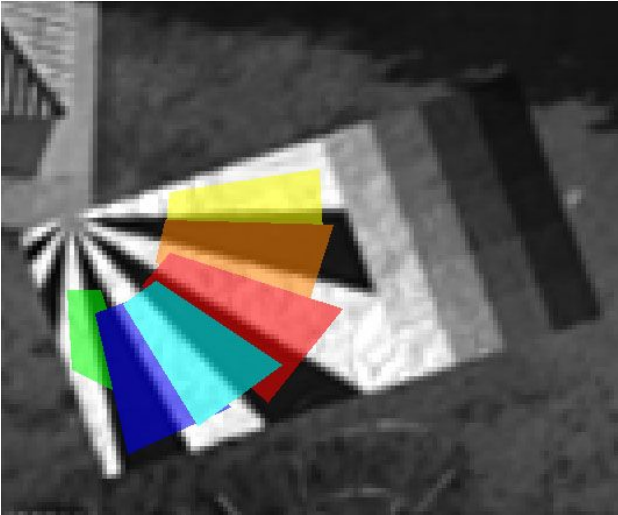

Figure 4. Digital image of the target with manual polygons superimposed

Next, a 5-parameter, 3-D sigmoid is adjusted in an approach similar to that in (Blonski, 2001) or (Blonski et al. 2002). In our case, the form of the function is

$$f(j,i) = P_4 + \frac{P_1}{1 + e^{-P_3 \cdot (i \cdot \cos P_5 + j \cdot \sin P_5 - P_2)}} \qquad (1)$$

The derivative of this function can be considered as the Point Spread Function (PSF) of the system. The Full Width at Half Maximum (FWHM hereafter) of this PSF will be taken as a resolution measure (Perko et al., 2004).

Note that, although there is some controversy over which is the best definition of resolution for an image formation system, the aim here is to measure a ratio between both values in order to compare the performance of the cameras.

We can express the PSF as

$$f'(\gamma) = \frac{P_1 \cdot P_3 \cdot e^{-\gamma}}{(1 + e^{-\gamma})^2} \qquad (2)$$

where
$$\gamma = P_3 \cdot (-\beta - P_2)$$
$$\beta = i \cdot \cos P_5 - j \cdot \sin P_5$$

It is easy to follow that FWHM will only depend on P_3 taking, approximately, the value

$$FWHM \approx \frac{3.52549434807817}{P3} \qquad (3)$$

Parameter P_5 corresponds to the angle of the edge and will also be taken in account into the test.
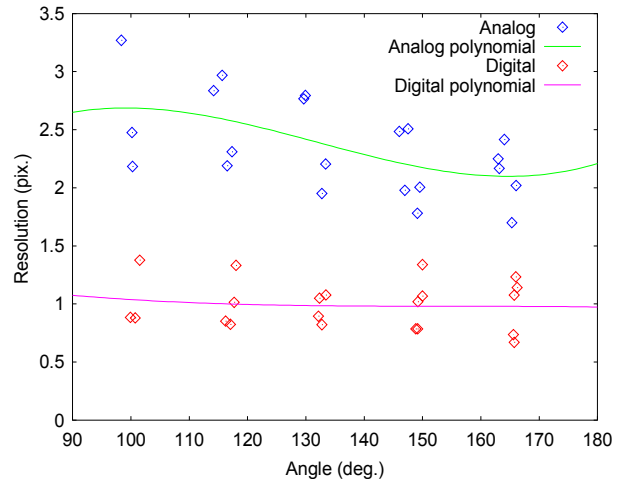

Figure 5. Measurements of resolution and fitted polynomials for analog (blue and green) and digital images (red and pink) against angle in image.

In figure 5 the obtained resolution values are plotted against the angle of the edge in the image. The first thing to notice is the difference in resolution between both cameras. In the most favorable case, a factor two in resolution against analog camera is obtained. Moreover, the resolution in the digital camera seems to remain approximately constant over different edge angles (no FMC effect) whereas in the analog case FMC inaccuracies and/or different scanner response in along- and across-swath directions combine to degrade resolution. Notice that 90 degrees is the direction of flight: along-track. So 180 degrees is across-track direction.

3.5 Notes on image quality

The DMC major advantage, in comparison with film cameras, is the fact that film developing and scanning steps are avoided. So, the process of aerial photography makes a further approach in the accomplishment of the fast mapping concept, providing access to digital images within a few hours delay instead of weeks. At the same time, the often required manual cosmetic task is simplified or reduced since no artifacts as scratches or dust are introduced during the film handling and scanning. Although dead or weak pixels are digital-inherent artifacts for

the CCDs, its influence in the orthoimage generation process is less important since their positions are well known from the calibration and, in consequence, they don't require additional manual work. Also an important and positive aspect is the simultaneous acquisition of B/W (high resolution), color and infrared (both at low resolution) image that, in the past, was only possible using two or three analog cameras operating simultaneously. Also to be highlighted is the 12-bit pixel radiometric resolution obtained for all the spectral components.

On the other hand, the major disadvantage or aspect to be enhanced in some way is the B/W full-frame reconstruction from the overlapping individual CCDs. The mosaicking process takes advantage of the platform calibration results and combines the four panchromatic images into a single DMC image. However, the maximum radiometric differences allowed among the four panchromatic images before mosaicking is a ±2 ‰ of the dynamic range. This translates to ±8 gray values that sometimes could make the mosaic evident. A high resolution RGB image is the result of combining the high resolution panchromatic image with the low resolution color image through a Pan-Sharpening process. The selected procedure is the RGB to HSL transformation and it can introduce some color artifacts that are visible only at a high zoom factor.

Also important to be taken into account is the lack of long term experience about the sensor stability, both from the geometric and radiometric point of view. Nevertheless, some experiments have been performed in that sense, which provide results similar to those with analog cameras. A totally pending issue is a systematic, precise radiometric calibration for the sensor. Working in that direction would permit to manage the color processing and the atmospheric corrections in a more rigorous way.

4. CONCLUSIONS

The evaluation tests have shown that the point accuracy of the DMC is comparable with analog cameras. Current results in aerotriangulation and setereoplotting pointing accuracy corroborate Dörstel's referenced papers. Nevertheless, it has to be investigated in further analysis whether DMC accuracy can be improved using a suitable set of self-calibration parameters in the bundle block adjustment.

Concerning DSM accuracy, it seems that DMC overcomes the handicap of the b/h ratio with its higher point accuracy in mountainous areas and it is barely noticeable in flat areas. Unluckily, data sets under study does not allow reach any final conclusion.

In most of the tests, stereoplotting with the DMC reaches comparable accuracy with film cameras. But results on measured height of adjacent across-track models show larger differences in the case of the DMC that can be improve by the above mentioned self-calibration parameters. Nevertheless, these results are not conclusive.

Further work should complete the studies on DSM generation and height accuracy in stereoplotting.

It has been proved that DMC resolution is about constant across the image and twice times better than analog cameras scanned at 15 μm. This fact, already known, allows DMC to compensate the poorer ratio b/h (by a factor of two compared to the analog cameras).

Concerning image quality, DMC provides well-known advantages as a quicker availability of images, the drastic reduction of artifacts (scratches, dust, …) and 12-bit pixel radiometric resolution. Despite the good performance of the camera there are still some image effects that could and should be improved in next DMC software releases and, eventually, calibration procedures.

As an overall conclusion the DMC shows big improvements in some parts of the photogrammetric workflow while maintains the metric accuracy of the current analog cameras. Therefore, the camera has been accepted and put into production.

REFERENCES

Baron, A., Kornus, W., Talaya, J., 2003. ICC experiences on Inertial/GPS Sensor Orientation. In: *ISPRS WG I/5 Workshop "Theory, Technology and Realities of Inertial/GPS sensor orientation"*. 22-23rd September 2003, Castelldefels (Spain).

Blonski, S. 2001. Spatial Resolution of IKONOS Pan. Images: Characterization Based on Edge Responses. In: *2001 High Spatial Resolution Commercial Imagery Workshop*, 19-22nd March 2001, Greenbelt, MD (USA).

Blonski, S., Pagnutti, M., Ryan, R. E. and Zanoni, V., 2002. In-flight edge response measurements for high spatial- resolution remote sensing systems. In: *W. L. Barnes (ed.), Proceedings of SPIE: Earth Observing Systems VII*, Vol. 4814, pp. 317–326.

Colomina, I., Navarro, J., Termens, A., 1992. GeoTeX: A general point determination system. In: *Proceedings of the IntArchPhRs*, Com. II, Vol XXIX, pp 656-664.

Dörstel, C., 2003. DMC- Practical Experiences and Photogrammetric System Performance. In: *Photogrammetric Week 2003* Fritsh D. (Ed.), September 2003 Sttutgart (Germany), pp. 59-65.

Dörstel, C., Jacobsen, K., Stallmann, D., 2003. DMC - Photogrammetric Accuracy – Calibration aspects and generation of synthetic DMC images. In: *Grün A., Kahmen H.(Eds.) Optical 3-D Measurement Technics VI*, Vol. I, Intitut fot Geodesy and Photogrammetry, ETH, Zürich, pp 74-88.

Ebner, H., 1976. Self-calibrating block adjustment. In: *Congress of the International Society for Photogrammetry.* Invited paper of Commission III, 1976, Helsinki (Finland).

Krzystek P., 1991. Fully Automatic Measurement of Digital Elevation Models. In: *Proceedings of the 43th Photogrammetric Week.* 1991, Stuttgart (Germany), pp. 203-214.

Perko, R., Klaus A., Gruber M., 2004 Quality Comparison of Digital and Film-based Images for Photogrammetric Purposes. In: *Proceedings of the XXth ISPRS Congress*, 12-23rd July 2004, Istambul (Turkey).

Zeitler, W., Dörstel, C., Jacobsen, K., 2002. Geometric Calibration of the DMC: Method and Results. In: *IntArchPhRs*, Com. I, Denver (USA), Vol XXXIV Part 3b, pp 324-333.